



X-ray–optical cross-correlator for gas-phase experiments at the Linac Coherent Light Source free-electron laser

S. Schorb, T. Gorkhover, J. P. Cryan, J. M. Glowina, M. R. Bionta, R. N. Coffee, B. Erk, R. Boll, C. Schmidt, D. Rolles, A. Rudenko, A. Rouzee, M. Swiggers, S. Carron, J.-C. Castagna, J. D. Bozek, M. Messerschmidt, W. F. Schlotter, and C. Bostedt

Citation: [Applied Physics Letters](#) **100**, 121107 (2012); doi: 10.1063/1.3695163

View online: <http://dx.doi.org/10.1063/1.3695163>

View Table of Contents: <http://scitation.aip.org/content/aip/journal/apl/100/12?ver=pdfcov>

Published by the [AIP Publishing](#)

Articles you may be interested in

[Spectral encoding method for measuring the relative arrival time between x-ray/optical pulses](#)

Rev. Sci. Instrum. **85**, 083116 (2014); 10.1063/1.4893657

[An extreme ultraviolet Michelson interferometer for experiments at free-electron lasers](#)

Rev. Sci. Instrum. **84**, 095111 (2013); 10.1063/1.4821146

[Femtosecond synchronism of x-rays and visible/infrared light in an x-ray free-electron laser](#)

Rev. Sci. Instrum. **78**, 123302 (2007); 10.1063/1.2805114

[Femtosecond synchronism of x rays to visible light in an x-ray free-electron laser](#)

Rev. Sci. Instrum. **76**, 063304 (2005); 10.1063/1.1927109

[The coherent light source project at SLAC](#)

AIP Conf. Proc. **525**, 623 (2000); 10.1063/1.1291979

A promotional banner for Applied Physics Reviews. On the left is a small image of a journal cover titled 'AIP Applied Physics Reviews' featuring a diagram of a crystal structure. The main background is dark blue with a bright light source on the right. The text 'NEW Special Topic Sections' is prominently displayed in white. Below this, it says 'NOW ONLINE' in yellow, followed by 'Lithium Niobate Properties and Applications: Reviews of Emerging Trends' in white. The AIP Applied Physics Reviews logo is in the bottom right corner.

NEW Special Topic Sections

NOW ONLINE
Lithium Niobate Properties and Applications:
Reviews of Emerging Trends

AIP Applied Physics
Reviews

X-ray–optical cross-correlator for gas-phase experiments at the Linac Coherent Light Source free-electron laser

S. Schorb,¹ T. Gorkhover,² J. P. Cryan,¹ J. M. Glowia,¹ M. R. Bionta,¹ R. N. Coffee,¹ B. Erk,^{3,4} R. Boll,^{3,4} C. Schmidt,^{3,4} D. Rolles,^{3,5} A. Rudenko,^{3,4} A. Rouzee,⁶ M. Swiggers,¹ S. Carron,¹ J.-C. Castagna,¹ J. D. Bozek,¹ M. Messerschmidt,¹ W. F. Schlotter,¹ and C. Bostedt^{1,a)}

¹Linac Coherent Light Source, SLAC National Accelerator Laboratory, P.O. Box 20450, Stanford, California 94309, USA

²Institut für Optik und Atomare Physik, Technische Universität Berlin, Hardenbergstr. 36, 10623 Berlin, Germany

³Max-Planck Advanced-Study-Group at CFEL, Notkestr. 85, 22607 Hamburg, Germany

⁴Max-Planck-Institut f. Kernphysik, Saupfercheckweg 1, 69117 Heidelberg, Germany

⁵Max-Planck-Institut f. med. Forschung, Jahnstr. 29, 69120 Heidelberg, Germany

⁶Max-Born-Institut, Max-Born-Str. 2, 12489 Berlin, Germany

(Received 5 January 2012; accepted 26 January 2012; published online 20 March 2012)

X-ray–optical pump–probe experiments at the Linac Coherent Light Source (LCLS) have so far been limited to a time resolution of 280 fs fwhm due to timing jitter between the accelerator-based free-electron laser (FEL) and optical lasers. We have implemented a single-shot cross-correlator for femtosecond x-ray and infrared pulses. A reference experiment relying only on the pulse arrival time information from the cross-correlator shows a time resolution better than 50 fs fwhm (22 fs rms) and also yields a direct measurement of the maximal x-ray pulse length. The improved time resolution enables ultrafast pump–probe experiments with x-ray pulses from LCLS and other FEL sources. © 2012 American Institute of Physics. [<http://dx.doi.org/10.1063/1.3695163>]

Femtosecond x-ray pulses from free-electron laser (FEL) sources such as the Linac Coherent Light Source (LCLS)¹ hold great promise for investigating the dynamics of chemical reactions and materials. They allow the application of x-ray based tools for element-specific spectroscopy as well as imaging with atomic resolution in a time-resolved manner. In these experiments, typically a system is pumped with an optical laser and its time evolution is probed with the fs x-ray pulses.

The synchronization between the particle accelerator based FEL and the optical laser poses a major challenge. The arrival times of the electron bunches exhibit a jitter with respect to the accelerator radio frequency, making perfect synchronization of both lasers virtually impossible. To overcome the jitter, there exist two general strategies. In the first one, the arrival times of the electron bunches are measured by either electro-optical sampling² or phase cavities³ and the data is corrected with the timing information. While the electron arrival time can be measured with few ten fs precision, other timing uncertainties are introduced by the large distance between the electron arrival time measurement and the experiment. The best resolution so far achieved at LCLS with this approach is on the order of 280 fs full-width-at-half-maximum (fwhm).³

The other strategy is to directly measure the relative arrival time of both laser pulses at the experiment. The techniques for cross-correlation of an x-ray and optical laser pulse, however, are much less mature and still a topic of active research. So far, great progress has been made with intense short-wavelength pulses in the extreme vacuum ultraviolet

spectral regime from the FLASH FEL.⁴ First experiments have utilized sidebands from two-photon above threshold ionization of atomic targets to characterize the temporal jitter between the FEL and optical pulses.^{5,6} For the hard x-ray regime strong field ionization of atomic targets opening resonant absorption channels has been proposed as x-ray–optical cross correlation technique.⁷ Alternative approaches to two-color ionization of atomic targets are to measure ultrafast x-ray induced changes in surface reflectivity⁸ or transient changes in the optical transmission of a membrane via spectral encoding.⁹ Based on the tilted wavefront technique,¹⁰ the reflectivity method has been further developed into a single-shot measurement of the relative timing between short wavelength pulses from the FLASH free electron and an external optical laser.¹¹

We have implemented an optical–x-ray cross-correlator based on surface reflectivity changes at the Atomic, Molecular, and Optical (AMO) physics endstation¹² of the LCLS. The cross-correlator is mounted downstream of the main experiment preserving the full x-ray beam for thin-target experiments in the interaction region, as opposed to an upstream setup at the soft x-ray and materials science (SXR) beamline optimized for solid sample experiments.¹³ Using only the timing information from the cross-correlator, we demonstrate a time resolution in a x-ray pump–optical probe reference experiment of better than 50 fs fwhm or 22 fs root-mean-square (rms). The experimental setup is depicted in Fig. 1. The FEL beam is focussed in the interaction region of the CAMP endstation¹⁴ for the timing reference experiment and the x-ray–optical cross-correlator is mounted downstream. An 800 nm near-infrared (NIR) beam is split and sent to both, the cross-correlator and the reference experiment. The two NIR laser pulses are separately compressed to

^{a)}Author to whom correspondence should be addressed. Electronic mail: bostedt@slac.stanford.edu.

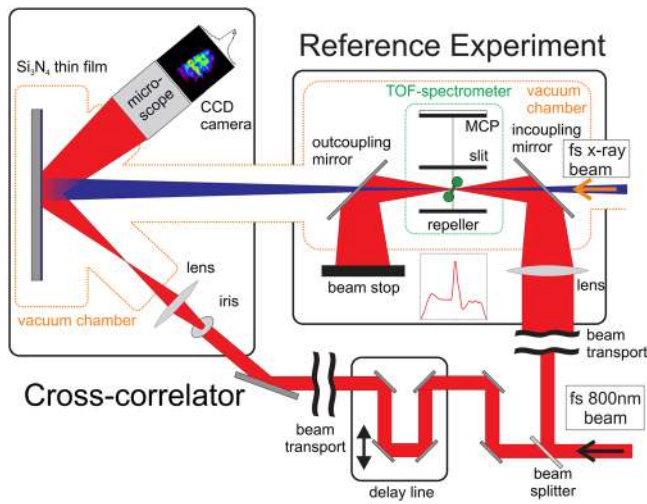


FIG. 1. (Color online) Right: Setup of the nitrogen ionization reference experiment. The FEL and NIR beam are focussed over the entrance aperture of a tof spectrometer. Left: Cross-correlator downstream of the reference experiment. The FEL comes in normal to the Si_3N_4 surface with a footprint of 1.3 mm. An iris in the NIR beam is imaged onto the surface and overlapped with the x-ray spot. The reflection is imaged via a long distance microscope onto a CCD camera.

a pulse length of 50 fs and their relative timing is adjusted with a delay stage. In the cross-correlator, the relative timing between the NIR and x-ray pulses is measured on a shot-by-shot basis. The 800 nm laser beam is reflected off a 100 nm Si_3N_4 film on a Si substrate under an angle of 40° to the surface normal. The spot of the NIR pulse is imaged with a long-distance microscope on a CCD camera. The x-rays come in normal to the surface and are overlapped with the NIR beam. The relative timing of the laser pulses is encoded in the spatial position of the x-ray induced reflectivity change of the surface.

The timing information from the cross-correlator is referenced to the NIR induced dissociation of x-ray produced doubly charged nitrogen molecules³ measured in an inde-

pendent experiment running simultaneously in the FEL focus upstream of the cross-correlator. In the reference experiment, the NIR is propagated collinearly to the x-ray beam and both foci are overlapped above the entrance slit of a time-of-flight (tof) ion spectrometer. The FEL pulse parameters are a photon energy of 1.7 keV with an average pulse energy of 2 mJ and an electron bunch length of 95 fs. All data are acquired on a shot-by-shot basis and correlated to the beam parameters.

The regions of interest of four typical cross-correlator single-shot images are shown in the top panels of Fig. 2. All images are normalized with an averaged NIR-only reference. The onset of the x-ray induced reflectivity change can be clearly seen as an edge which moves as a function of relative delay. The structure in the four images stems from intensity variations in the FEL beam profile. The edge exhibits a 4° angle with respect to the horizontal due to a slight rotation of the CCD camera. The bottom of Fig. 2 shows the projections of the images onto a line perpendicular to the edge of the reflectivity change, i.e., taking into account this 4° angle. The data show a strong increase of the reflectivity of roughly 40%. The Si_3N_4 thin film acts akin an anti-reflective coating leading to destructive interference between the NIR beams reflected from the front and back of the film. The refractive index n of the Si_3N_4 determines the phase relation between the two NIR beams and even slight variations in n stemming from the x-ray induced carrier dynamics lead to the observed increase in reflectivity. The relative timing of the NIR and x-ray laser pulses has been obtained from the projections of the edge using a constant fraction type algorithm. It is interesting to note that the projection slightly smears out the rise time of the edge due to the variations in the FEL beam profile but leads to more reliable edge finding results without jeopardizing the timing information. Single line-outs exhibit a rise time of ≈ 65 fs which is similar to the x-ray pulse length as discussed below. This indicates that the x-ray induced carrier dynamics responsible for the change in refractive index happen on the femtosecond time scale.¹⁵

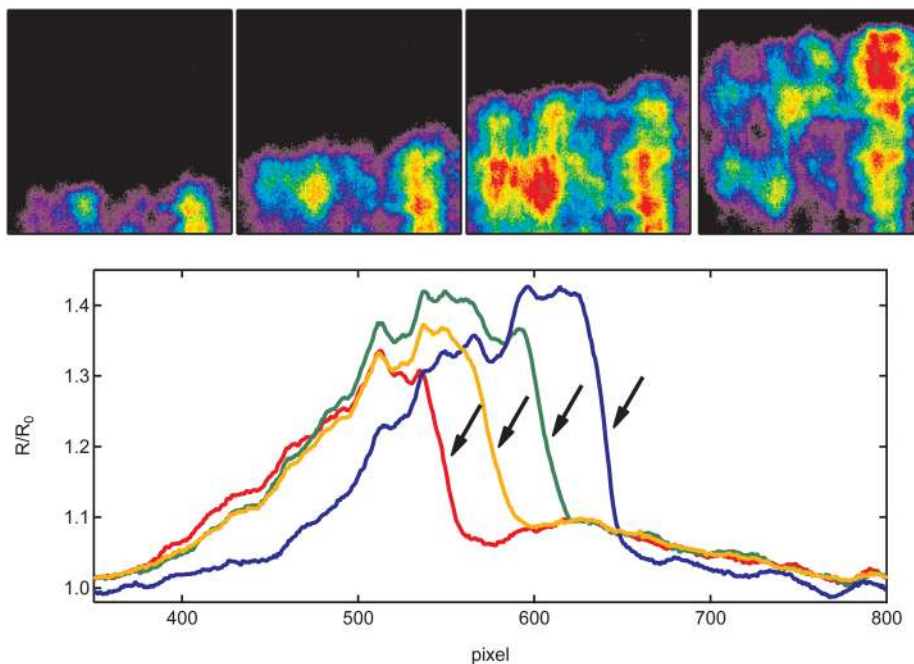


FIG. 2. (Color online) Top: Region of interest of four single shot images recorded by the CCD camera in the cross-correlator. The onset of the x-ray induced reflectivity change moves with the varying relative arrival times. Bottom: Projections of the above images along the edge. The arrows indicate the relative pulse arrival time determined by the constant fraction type algorithm. All data are normalized with an averaged NIR-only signal R_0 .

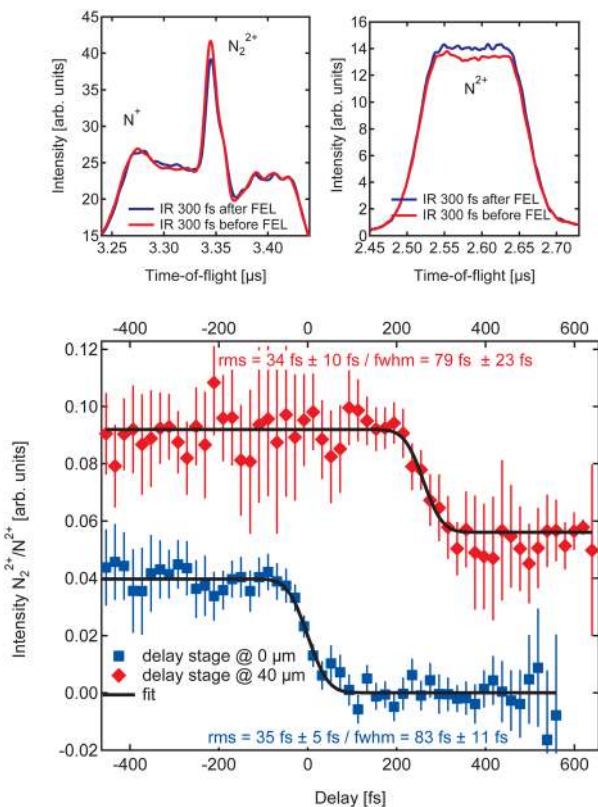


FIG. 3. (Color online) Top: N_2^{++} and N_2^+ contributions of the tof spectrum for NIR before x-ray and NIR after x-ray pulse. Bottom: N_2^{++}/N_2^+ signal plotted vs. the relative arrival times of the x-ray and NIR pulses obtained from the cross-correlator. The two curves are measured for different delay stage settings and the upper curve is shifted in x for better visibility. The curves have been independently fitted with the integral of a Gaussian (error function).

The nitrogen reference data recorded with a chamber backfilled to approximately 10^{-6} mbar N_2 is shown in the top panel of Fig. 3. Doubly charged N_2^{++} molecules can be created by the x-ray pulse through core-ionization and subsequent Auger decay with a lifetime of 6.4 fs.¹⁶ The quasi-bound states of N_2^{++} can then be dissociated by the intense NIR laser pulse,¹⁷ yielding a reliable method to determine whether the NIR arrived before or after the x-ray pulse.³ Comparing the spectra taken with the NIR 300 fs before and after the x-ray pulse mainly a depletion of the N_2^{++} with a

simultaneous increase of N_2^+ is observed, indicating a dissociation into a doubly charged and neutral nitrogen atom.

In the bottom panel of Fig. 3, the intensity ratios of N_2^{++} to N_2^+ is plotted, using only the relative pulse arrival time information from the cross-correlator. Each of the curves has been acquired by collecting data with the natural jitter of the FEL at three different electronic delays of $\Delta T = 250$ fs. The data are then sorted in the post-analysis according to the edge positions in the cross-correlator. Additionally, the delay stage between both NIR arms has been moved by $40 \mu\text{m}$ (264 fs) in order to calibrate the setup (6.75 fs per pixel) and to measure the x-ray–NIR delay on two different surface spots. The blue curve in Fig. 3 exhibiting better statistics can be fit with an integrated Gaussian (error function) to $\approx 83 \pm 11$ fs fwhm.

The width of the fitted error function is a convolution of the temporal profiles of the x-ray pulse, the NIR pulse, and the intrinsic resolution of the cross-correlator. The time constant of creation and dissociation of the N_2^{++} molecule is much shorter than the laser pulse lengths and therefore is neglected in the following discussion. Considering that the NIR pulse is 50 fs, the current measurement directly shows that the x-ray pulse is significantly shorter than the electron bunch length of 95 fs, in agreement with the predictions from the first experiments at LCLS.¹⁸ A recent combined experimental and theoretical study shows the x-ray pulse length to be about 68% of electron bunch length,¹⁹ translating to a 65 fs x-ray pulse for the current experiment. The time constants of the rising edges in Fig. 3 are well described by the convolution of the temporal profiles of both lasers ($T_{edge} = \sqrt{65^2 + 50^2} = 82$ fs), assuming Gaussian envelope functions for the laser pulses. Therefore, the current measurement is predominantly limited by the pulse lengths of both lasers and it sets an upper limit for the time resolution to the error of the fits in Fig. 3 to $T_{resolution} < \sqrt{(83 + 11)^2 - 65^2 - 50^2} \approx 50$ fs.

In Fig. 4(a), the correlation between the edge position derived from two different areas of the x-ray spot is shown. The deviation of the points from the diagonal is a measure for the uncertainty of the edge finding due to the spatial intensity profile of the x-ray beam. Fig. 4(b) shows the projection of different regions of this correlation plot along the diagonal. Over the whole measurement range of 1000 fs, this

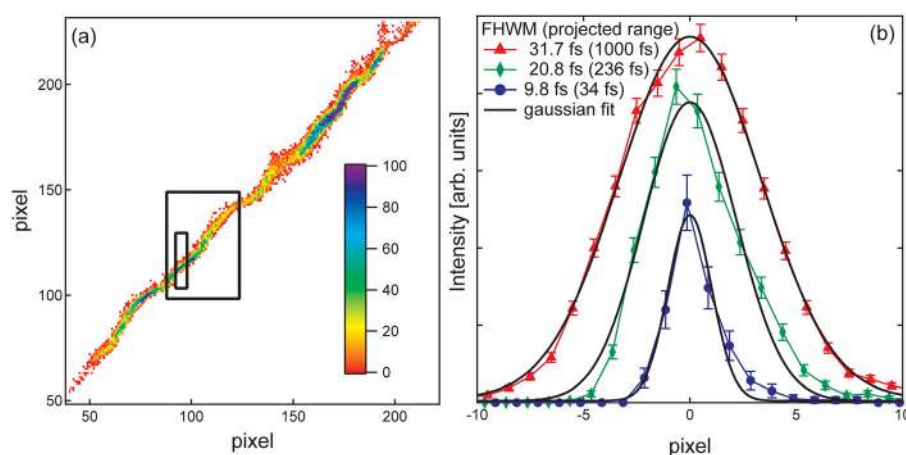


FIG. 4. (Color online) (a) Correlation plot for the edge positions from two different areas on the x-ray spot. (b) Projection of (a) along the diagonal for the full measurement range (red triangles), 35 pixels (green diamonds), and 5 pixel (blue circles) corresponding to the full graph, the big box, and the small box in the left panel, respectively.

uncertainty accounts for an error of 32 fs fwhm in timing the x-ray and NIR pulses. The edge finding variation becomes smaller when the measurement is limited to a smaller area on the substrate, i.e., when a more constant spatial intensity profile of the x-ray beam is used. With these restrictions, it can be as low as 10 fs fwhm for a 34 fs (five pixel) window. Thus, in order to perform ultra-high time resolution experiments, the data collection scheme would need to be changed so that the delay stage between both laser pulses is moved and always the same area within the x-ray spot is used for the cross correlation.

In conclusion, we have measured the relative arrival times of femtosecond optical and keV x-ray pulses on a shot-by-shot basis by means of x-ray induced surface reflectivity changes. The temporal response of the Si₃N₄ surface is comparable to the x-ray pulse length. An independent reference experiment relying only on the time information from the cross-correlator demonstrates a time resolution of better than 50 fs fwhm (22 fs rms) and yields a direct measurement of the maximal x-ray pulse length. This dramatically improved time resolution will allow investigating optically induced ultrafast processes with x-ray free-electron sources.

This research was carried out at the Linac Coherent Light Source (LCLS) at SLAC National Accelerator Laboratory. LCLS is an Office of Science User Facility operated for the U.S. Department of Energy Office of Science by Stanford University.

¹P. Emma, R. Akre, J. Arthur, R. Bionta, C. Bostedt, J. Bozek, A. Brachmann, P. Bucksbaum, R. Coffee, F. J. Decker *et al.*, *Nat. Photonics* **4**, 641 (2010).

²A. L. Cavalieri, D. M. Fritz, S. H. Lee, P. H. Bucksbaum, D. A. Reis, J. Rudati, D. M. Mills, P. H. Fuoss, G. B. Stephenson, C. C. Kao *et al.*, *Phys. Rev. Lett.* **94**, 114801 (2005).

³J. M. Glowina, J. P. Cryan, J. Andreasson, A. Belkacem, N. Berrah, C. I. Blaga, C. Bostedt, J. D. Bozek, L. F. DiMauro, L. Fang *et al.*, *Opt. Express* **18**, 17620 (2010).

⁴W. Ackermann, G. Asova, V. Ayvazyan, A. Azima, N. Baboi, J. Baehr, V. Balandin, B. Beutner, A. Brandt, A. Bolzmann *et al.*, *Nat. Photonics* **1**, 336 (2007).

⁵P. Radcliffe, S. Düsterer, A. Azima, H. Redlin, J. Feldhaus, J. Dardis, K. Kavanagh, H. Luna, J. P. Gutierrez, P. Yeates *et al.*, *Appl. Phys. Lett.* **90**, 131108 (2007).

⁶S. Cunovic, N. Müller, R. Kalms, M. Krikunova, M. Wieland, M. Drescher, Th. Maltezopoulos, U. Frühling, H. Redlin, E. Plönjes-Palm *et al.*, *Appl. Phys. Lett.* **90**, 121112 (2007).

⁷B. Krässig, R. W. Dunford, E. P. Kanter, E. C. Landahl, S. H. Southworth, and L. Young, *Appl. Phys. Lett.* **94**, 171113 (2009).

⁸C. Gahl, A. Azima, M. Beye, M. Deppe, K. Doebrich, U. Hasslinger, F. Hennies, A. Melnikov, M. Nagasono, A. Pietzsch *et al.*, *Nat. Photonics* **2**, 165 (2008).

⁹M. R. Bionta, H. T. Lemke, J. P. Cryan, J. M. Glowina, C. Bostedt, M. Cammarata, J.-C. Castagna, Y. Ding, D. M. Fritz, A. R. Fry *et al.*, *Opt. Express* **19**, 21855 (2011).

¹⁰K. Sokolowski-Tinten, A. Cavalleri, and D. von der Linde, *Appl. Phys. A* **69**, 577 (1999).

¹¹T. Maltezopoulos, S. Cunovic, M. Wieland, M. Beye, A. Azima, H. Redlin, M. Krikunova, R. Kalms, U. Frühling, F. Budzyn *et al.*, *New J. Phys.* **10**, 033026 (2008).

¹²J. D. Bozek, *Eur. Phys. J.* **169**, 129 (2009).

¹³M. Beye, O. Krupin, G. Hays, A. H. Reid, D. Rupp, S. de Jong, S. Lee, W.-S. Lee, Y. D. Chuang, C. Bostedt *et al.*, *Appl. Phys. Lett.* **100**, 121108 (2012).

¹⁴L. Strüder, S. Eppa, D. Rolles, R. Hartmann, P. Holl, G. Lutz, H. Soltau, R. Eckart, C. Reich, K. Heinzinger *et al.*, *Nucl. Instrum. Methods Phys. Res. A* **614**, 483 (2010).

¹⁵B. Ziaja, R. A. London, and J. Hajdu, *J. Appl. Phys.* **97**, 064905 (2005).

¹⁶B. Kempgens, A. Kivimaki, M. Neeb, H. M. Koppe, A. M. Bradshaw, and J. Feldhaus, *J. Phys. B* **29**, 5389 (1996).

¹⁷R. N. Coffee, L. Fang, and G. N. Gibson, *Phys. Rev. A* **73**, 043417 (2006).

¹⁸L. Young, E. P. Kanter, B. Krässig, Y. Li, A. M. March, S. T. Pratt, R. Santra, S. H. Southworth, N. Rohringer, L. F. DiMauro *et al.*, *Nature* **466**, 56 (2010).

¹⁹S. Düsterer, P. Radcliffe, C. Bostedt, J. Bozek, A. L. Cavalieri, R. Coffee, J. T. Costello, D. Cubaynes, L. F. DiMauro, Y. Ding *et al.*, *New J. Phys.* **13**, 093024 (2011).